Single and Multiple Longitudinal Wavelength Generation in Green Diode Lasers

Md Hosne Mobarok Shamim, Tien Khee Ng, *Senior Member, IEEE*, Boon S. Ooi, *Senior Member, IEEE*, and Mohammed Zahed Mustafa Khan, *Senior Member, IEEE*

***Abstract*—Single and multiple wavelength laser systems are presented that employ self-injection locked InGaN/GaN green laser diodes in an external cavity configuration with a partially reflective mirror. A stable and simultaneous locking of up to four longitudinal Fabry–Perot modes of the system cavity is demonstrated with appreciable signal-to-noise-ratio of ∼13 dB and average mode linewidth of ∼150 pm. The multi-wavelength spectrum exhibited a flat-top emission with nearly equal power distribution among the modes and an analogous mode spacing of ∼0.5 nm. This first demonstration of multi-wavelength generation source is highly attractive in a multitude of cross-disciplinary field applications besides asserting the prospects of narrow wavelength spaced multiplexed visible light communication. Moreover, an extended two-stage self-injection locked near single wavelength visible laser system is also presented. An ultra-narrow linewidth of ∼34 pm is realized at 525.05 nm locked wavelength from this innovative system, with ∼20 dB side-mode-suppression-ratio; thus signifying a paradigm shift toward semiconductor lasers for near single lasing wavelength generation, which is presently dominated by other kinds of laser technologies.**

***Index Terms*—External cavity diode laser, self-injection locking, visible multi-wavelength laser, single frequency laser.**

I. Introduction

VISIBLE single/multiple longitudinal wavelength sources are invaluable for various multi-disciplinary field applications [1]. In particular, they are indispensable sources in optical communications, medical diagnostics, optical cloaking, metrology, precision spectroscopy, bio-sensing, microwave photonics, etc. [2]. In literature, visible coherent single and multiple longitudinal wavelength emissions are demonstrated on external cavity diode laser (ECDL) system and semiconductor gain medium–optical fiber configuration, respectively. While the former technology employs a wavelength grating filtering mechanism for single wavelength selection, the latter technique exploits various non-linear phenomena to realize a coherent frequency comb or multi-wavelength generation. In the following, we briefly review these technologies.

ECDL system in Littrow configuration is one such system that has been used often in the visible wavelengths to realize single longitudinal wavelength emission as well as tunable lasers. For instance, Chen *et al.* demonstrated a single wavelength operation in green emission wavelength with ∼10 MHz linewidth [3]. Subsequently, a more stable system at ∼522 nm using iodine was demonstrated; however, at the cost of broader linewidth, in GHz range [4]. Moreover, green tunable laser in the range of 509–518 nm with ∼17 dB amplified spontaneous emission (ASE) suppression was also demonstrated using a similar configuration [5]. However, the Littrow configuration ECDL system suffers from high loss and alignment issues [6]. Very recently, a blue GaN distributed-feedback laser diodes have been reported using high order notch gratings to obtain single wavelength emission with a narrow linewidth of 6.5 pm and 35 dB side mode suppression ratio (SMSR) [2].

Incoherent and coherent multiple longitudinal wavelength emission in the form of frequency comb generation has been reported in AlN/SiN micro-resonators and optical fibers, respectively, employing non-linear effects. For instance, a highly coherent visible optical frequency comb spanning from 500 nm to 1200 nm was demonstrated from a 1550 nm Er-doped fiber laser using frequency double conversion [7]. 14 comb lines in visible wavelengths were demonstrated in a dispersion engineered fiber using four-wave mixing, phase matched at 765 nm [8]. However, to the authors' knowledge, multiple longitudinal wavelength generation from a visible diode laser has not been reported. Such a compact system has already attracted attention in the near infrared region (∼1300–1630 nm) with promising demonstrations in the microwave and terahertz optical beat frequency generation, indoor data center communication, and wavelength division multiplexed passive optical networks [9]– [12]. In this case, various nanostructures viz. quantum well [13], quantum dash [14]–[16], and quantum dot [17], [18] based lasers have been engaged. Hence, a compact coherent multiple wavelength visible laser diode with narrow and uniform

Manuscript received January 31, 2019; revised May 1, 2019; accepted May 8, 2019. Date of publication May 15, 2019; date of current version June 4, 2019. This work was supported in part by the King Abdulaziz City for Science and Technology (KACST) under Grants EE2381 and KACST TIC R2-FP-008, in part by King Abdullah University of Science and Technology (KAUST) baseline funding under Grants BAS/1/1614-01-01, KCR/1/2081-01-01, and GEN/1/6607-01-01, and in part by KAUST-KFUPM Special Initiative (KKI) Program (REP/1/2878-01-01). *(Corresponding author: Mohammed Zahed Mustafa Khan.)*

M. H. M. Shamim was with the Optoelectronic Research Laboratory Department of Electrical Engineering, King Fahd University of Petroleum and Minerals, Dhahran 31261, Saudi Arabia. He is now with the Department of Electrical and Computer Engineering, McGill University, Montreal, QC H3A 0G4, Canada (e-mail: hosne.shamim@mail.mcgill.ca).

T. K. Ng and B. S. Ooi are with Photonics Laboratory, Computer, Electrical and Mathematical Sciences and Engineering (CEMSE) Division, King Abdullah University of Science and Technology, Thuwal 23955-6900, Saudi Arabia (e-mail: tienkhee.ng@kaust.edu.sa; boon.ooi@kaust.edu.sa).

M. Z. M. Khan is with the Optoelectronic Research Laboratory, Department of Electrical Engineering, King Fahd University of Petroleum and Minerals, Dhahran 31261, Saudi Arabia (e-mail: zahedmk@kfupm.edu.sa).

Color versions of one or more of the figures in this paper are available online at http://ieeexplore.ieee.org.

Digital Object Identifier 10.1109/JSTQE.2019.2916870

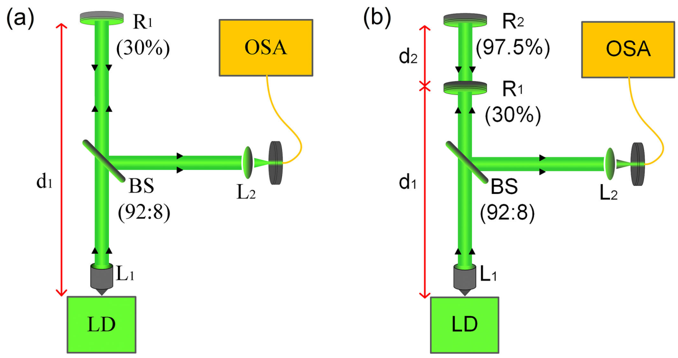

Fig. 1. Block diagrams of (a) single stage (for tunable laser and multi-wavelength generation) and (b) two-stage (near single wavelength generation) self-injection locked laser system employing InGaN/GaN green laser diode.

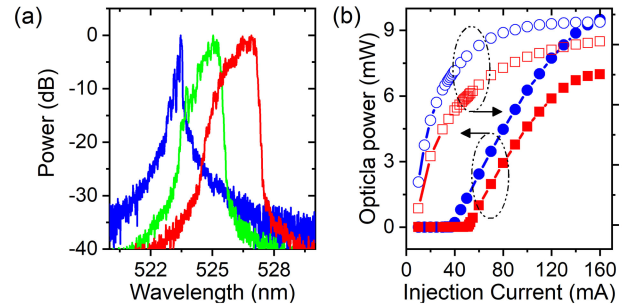

Fig. 2. (a) The free running optical spectrums of the laser diode at 40 (blue), 90 (green), 160 (red) mA recorded at 20 °C temperature. (b) *L-i-V* characteristics of the free running laser diode at 20 °C (blue) and 40 °C (red) temperature, measured after L_2.

wavelength spacing is of paramount importance to facilitate high capacity wavelength division multiplexed visible light communication (WDM-VLC) system, which is considered as a viable last mile-access network infrastructure. Moreover, unlike the recent demonstration of WDM-VLC [19]–[22] links wherein wide wavelength spaced red-blue-green colors are employed as subcarriers, such a narrow-spaced multi-wavelength visible laser source based network architecture would enable optimization of the available optical bandwidth.

Very recently, we proposed a new-class of wavelength filterless ECDL system employing assisting self-injection locking scheme. By implicitly inheriting the distinct locking characteristics, we demonstrated narrow lasing emission linewidths of 70–120 pm on red, blue, and green color laser diodes [23]. Moreover, a wavelength tunability in the range of ~521–528 nm with high output power was also realized employing this configuration.

In this work, we further substantiate the potential of this new class of ECDL system as a viable solution for realizing high-performance visible laser diodes. Firstly, by employing a first-of-its-kind extended three-cavity ECDL system with two-stage self-injection locking, we demonstrate a single-wavelength operation at 525.05 nm with ~34 pm linewidth and ~20 dB SMSR. Secondly, a coherent, narrow-spaced, multiple longitudinal wavelength generation is realized with a two cavity self-injection locked ECDL system. By simultaneously locking up to 4 Fabry-Perot (FP) modes with ~0.5 nm spacing, a coherent frequency comb source is realized for the first time, to our knowledge, on a semiconductor diode laser based system in the visible wavelength. Mean linewidths of ~150 pm with an average ~15 dB SMSR is achieved with comparable peak and integrated powers, and stable operation.

II. Experimental Setup and Basic Laser Diode Characterization

The experimental setup for the multiple and single wavelength laser system is shown in Fig. 1(a) and (b), respectively. We have used a commercially available single spatial mode InGaN/GaN green laser diode LD (Thorlabs L520P50) as a source whose emission wavelength is in the range of 520–529 nm. The green laser beam is allowed to pass through an aspheric lens L_1 (Thorlabs, A110TM-A) and after being collimated, 92% of the light beam traveled through a 92:8 pellicle beam splitter (BS, Thorlabs, BP108). An external cavity resonator is formed between the front facet of the laser diode and the partial reflector R_1 (polka dot beam splitter from Edmund optics) with 30% reflectivity. R_1 is installed on a manual kinematic mount (Thorlabs, KM100) and single-axis translational stage, at the other end of the optical axis and a distance $d_1 = 26$ cm. Kinematic mounts enable slightly angular as well as linear tuning of the reflected beam and hence of the tuning of external cavity length is done. The other 8% reflected the light beam from the BS was coupled into an optical fiber through a biconvex lens L_2 (Thorlabs, LB1471-A-ML) of focal length 50 mm, for spectral analysis utilizing an optical spectrum analyzer (OSA, Yokogawa AQ6373B with 0.02 nm resolution). It is worth mentioning at this instant that the 70% of the transmitted power through R_1 appears as the output of the system that is ~ 65% of the laser diode optical power, thus reducing the system loss considerably. Besides, collection of the output power from the back facet of the laser diode would negate the loss of the power entirely.

Fig. 2(a) shows the lasing spectrums of the InGaN/GaN laser diode at 40, 90, and 160 mA injection currents spanning from just above the threshold to the maximum injection before the rollover with output power exceeding 10 mW. The −3 dB linewidths of the spectrums broaden gradually and redshifts, a legacy of bandgap shrinkage because of junction temperature rise due to an extreme surge of carriers. The threshold current of the laser diode is measured to be 37 and 47 mA at 20 and 40 °C, respectively, as observed from the *L-i-V* curves in Fig. 2(b). Moreover, at higher operating temperature, lower bias voltage and the emitted optical power with degraded slope efficiency are apparent across all the injection currents, which is attributed to the temperature-driven decrease of the internal quantum efficiency and the increase of the internal loss [25].

III. Narrow Linewidth Laser

A. Tunable Wavelength Generation

A two-cavity system as shown in Fig. 1(a) comprising the laser diode cavity and the external cavity allows longitudinal modes of different free spectral ranges. Locking of a specific

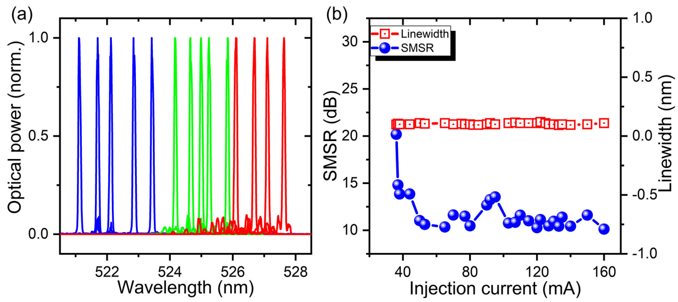

Fig. 3. (a) Overlapped lasing spectrums showing 6.53 nm discrete tunability of the system at 36, 95, and 160 mA injection current as shown in blue, green, and red color respectively. (b) SMSR and linewidth of the locked modes at various current injections as shown in blue spheres and red squares with a dot inside, respectively.

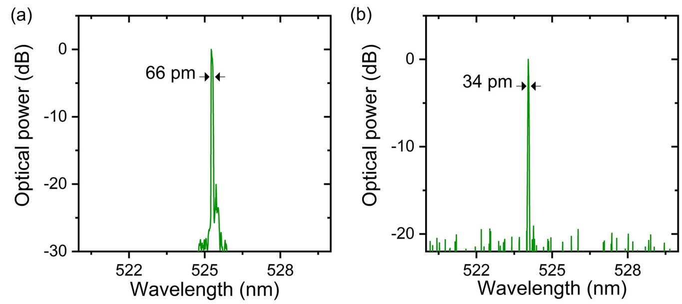

Fig. 4. Normalized optical lasing spectrums of single longitudinal mode with a very narrow linewidth of (a) 66 and (b) 34 pm, respectively. These values were recorded at 36 mA bias current and 20 °C temperature.

wavelengths using self-injection locking scheme takes place if the free spectral range (FSR) of the laser cavity is an integer multiple of that of the external cavity; in other word, round-trip phase matching condition should be satisfied. This phenomenon follows the relation between FSR and the cavity length as shown in (1).

$$\Delta\lambda_{FSR} = \lambda^2/2nL \quad (1)$$

Here, L represents the length of the cavities that are 900 μm and 26 cm (d_1) for the laser and external cavity, respectively. Hence, by careful tuning of the external cavity length via slight movement of tilt and linear stages, we were able to self-injection lock various modes of the laser diode and tune them discretely, as shown in Fig. 3(a). Near single longitudinal modes at different wavelengths in the range of 521.10 to 527.63 nm is apparent from the figure with a cumulative tunability of 6.53 nm that is obtained from three injection currents 36, 95, and 160 mA. The performance of the system is depicted in Fig. 3(b), which plots the achieved SMSR and the lasing linewidth (full-width-at-half-maximum) across the tuning window. SMSR as high as $\sim$20 dB is observed at the lower injection current and later saturates to $\sim$10 dB at high current injections. On the other hand, a steady linewidth of 100$\pm$20 pm is measured in the entire wavelength tuning range and is found to be independent of the injection current, thanks to the efficient locking at that particular wavelength. Moreover, the effect of temperature on the system demonstrated a robust and stable tunable laser system.

B. Single Wavelength Generation

Fig. 1(b) shows an extended three ECDL system to realize a single wavelength lasing operation. An additional reflector R_2 of reflectivity 97.5% (Thorlabs, PF10-03-P01) is placed after R_1 along the optical axis such that the distance $d_1 + d_2 = 26$ cm. In this case, R_1 is shifted closer towards the laser diode front facet and placed at a distance of $d_1 = 16$ cm. Hence, the composite cavity of the system now constitutes three FP resonators that include two external cavities of length d_1 and d_2. In this case, the usable output beam would be the reflected 8% from the BS that is used for diagnostic purpose. Since the reflected laser beam from two reflectors, R_1 and R_2, are optically feedback into the laser active region, the configuration is termed as two-stage self-injection locked external cavity laser system, and the first to be proposed and demonstrated here, to the authors' knowledge. A similar resonance frequency and phase matching conditions dictate this system, however, would be more stringent since here a particular mode from all the sustaining modes in the composite cavity should satisfy the phase matching condition in all the three FP cavities. In this configuration, by varying the position of R_1 tuning of both the external cavities is accomplished.

The threshold current in a self-injection locked laser diode reduces from its free running counterpart–a clear sign of locking phenomenon [24]. By executing a two-stage self-injection locking just below the threshold of the free running laser, at 36 mA, and 20 °C temperature, a narrow locked mode linewidth of $\sim$66 pm at 525.26 nm is obtained and depicted in Fig. 4(a). Furthermore, by careful and fine tuning of external cavity lengths, a linewidth of $\sim$34 pm at 524.05 nm is measured, as shown in Fig. 4(b). The latter measured value is two times narrower than the linewidth obtained in the tunable laser system employing single-stage self-injection locking. It is noteworthy to mention that the measured linewidth of $\sim$34 pm is smaller than the laser diode mode spacing of $\sim$60 pm suggesting a near single frequency operation. Besides, the measured linewidth is found to be near the resolution limit of the OSA ($\sim$20 pm), indicating a possibility of even narrower linewidth achievement by the system. Lastly, we noted that the stability of this two-stage self-injection locking system is comparatively inferior to that of the single-stage self-injection locking system of Fig. 1(a), which has been utilized for tunable as well as multi-wavelength generation. This is expected since fulfilling the stringent phase condition requirement with the manual tuning of this three-cavity system is non-trivial. Deployment of a piezo controlled tuning stage should enable achievement of stable operation from this system.

IV. MULTI-WAVELENGTH LASER

A. Dual Longitudinal Wavelength Generation

Employing the ECDL system shown in Fig. 1(a) with single-stage self-injection locking, we were able to lock two longitudinal modes simultaneously; a highly attractive scheme in microwave photonics for the optical generation of the millimeter

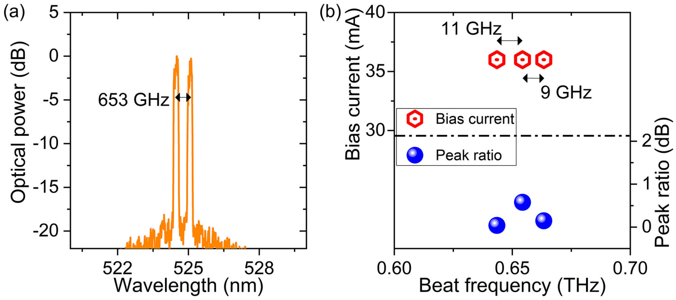

Fig. 5. (a) Normalized dual longitudinal mode operation generating 653 GHz of beat frequency and (b) beat frequencies generated at 36 mA bias current and the respective peak ratio of the modes.

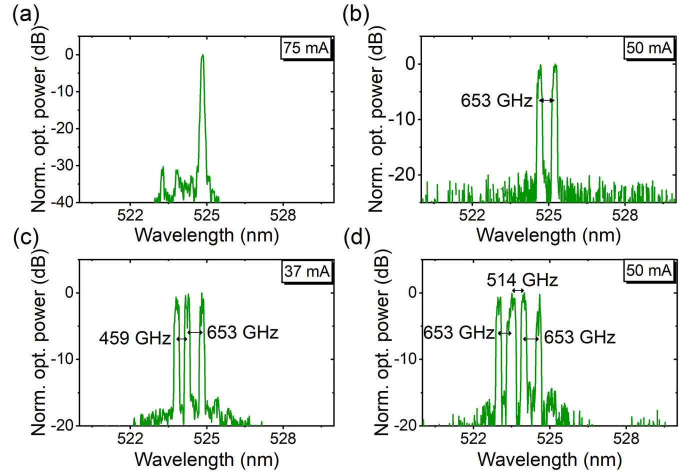

Fig. 6. Normalized multi-wavelength spectrums of self-injection locked external cavity system with simultaneous (a) single, (b) dual, (c) 3, and (d) 4 mode generation, at an injection current (temperature) of 75 mA (20 °C), 50 mA (40 °C), 37 mA (20 °C), and 50 mA (40 °C), respectively.

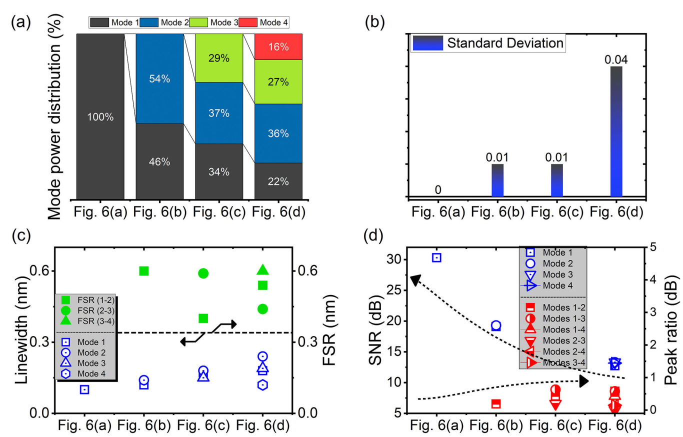

Fig. 7. (a) Optical power distribution, (b) standard deviation of the power distribution, (c) linewidth and FSR, and (d) SNR and peak power ratio of the individual longitudinal modes of various multi-wavelength spectrums of Fig. 6. The arrows in (c) and (d) are the guide to the eyes.

and terahertz beat frequencies (*i.e.,* the frequency difference between the two modes). Fig. 5(a) shows the two color locked spectrum with a mode spacing of ~0.6 nm, corresponding to ~653 GHz beat frequency, obtained at 36 mA injection current. Moreover, at the same biasing condition, on the further slight tuning of the external cavity length, the beat frequency could be altered to ~642, ~662 GHz and even higher values; a result of the change in the wavelength spacing between the two modes. These results are promising for tunable THz frequency wave generation in the optical domain. Moreover, in Fig. 5(b), the peak power ratio, which is the ratio of the peak powers of the two locked longitudinal modes, exhibited a value <0.6 dB implying almost equal peak as well as integrated power between the modes since a comparable modes linewidth of <200 pm is also observed. Furthermore, the peak to ASE ratio for both the modes is ~18 dB, an essential requirement for high-quality THz frequency generation. Observe that the usable optical power (after R_2) in this case is small owing to just above threshold current operation. Nonetheless, the optical power of the system could be improved significantly by biasing the laser diode at high current injection and employing high power watt level InGaN/GaN laser diode since dual locking is found to be nearly independent of operating current.

B. Multiple Longitudinal Wavelength Generation

By further careful tuning of the external cavity length, strikingly, the self-injection locked ECDL system (Fig. 1(a)) allowed simultaneous locking of 1 to 4 modes, as plotted in Fig. 6. This accomplishment ascertains that multiple frequency modes, which are comparatively closely spaced, could be phase-matched and locked simultaneously in the two-cavity system. Also, these multiple wavelength spectra displayed in Fig. 6, correspond to different injection currents and temperatures. For instance, multi-wavelength spectrums with 3 simultaneous locked FP modes is achieved at 37 mA bias current and 20 °C, whereas 4 such locked modes spectrum is obtained at 50 mA injection and 40 °C temperature. As discussed above, dual and even multi-wavelength locking is observed at all injection current and temperatures (independent of the diode laser operating conditions), so we selectively optimized few of them and presented in Fig. 6. This remarkable feature of our system not only assists in usable power enhancement but also indicates the flexibility and robustness of the configuration. Moreover, injection current and temperature could also serve as varying parameters in addition to the external cavity length, thereby offering an extra degree of freedom for simultaneous generation of several self-injection locked FP modes with uniform wavelength spacing and hence exhibiting multiple wavelength lasing characteristics.

Next, we analyze the performance of the multi-wavelength emission, firstly, by plotting in Fig. 7(a), the normalized integrated power distribution (in %) of each locked mode of Fig. 6 by neglecting the ASE noise. Evidently, 100% of the optical power in Fig. 6(a) is encompassed in the single locked mode while the power is almost equally distributed in dual lasing wavelength case of Fig. 6(b), which is estimated to be ~5.3 mW per mode and ~10.3 mW in total, measured at the output of R_1. In this case, the shorter and longer wavelength mode constitutes 54 and 46% of the total integrated power, respectively, with a corresponding minimal standard deviation of 0.01, as can be seen from Fig. 7(a) and (b). Considering the 3 frequency comb line spectrum, again a uniform ∼30% power distribution is observed across each mode with a uniform standard deviation of 0.01. However, this value increased to 0.04 for the comb source with 4 locked FP modes, suggesting a larger variation of the power distribution among the modes. Fig. 7(a) shows this uneven power distribution, with mode 2 and mode 4 exhibiting 37 and 16% of the total power, respectively. This is also reflected by the broad linewidth exhibited by mode 2 (∼240 pm) compared to other modes (mode 1: ∼180 pm, mode 3: ∼190 pm, and mode 4: ∼120 pm), as illustrated in Fig. 7(c). We postulate that in the 4 locked modes lasing spectrum, the complete gain profile might have been occupied by the longitudinal modes with lower power distributed to the two extreme modes (*i.e.,* 1 and 4), and hence resulting in smaller linewidth due to better localized injection ratio of these modes. On the other hand, the modes occupying the central part of the gain profile (*i.e.,* 2 and 3) probably exhibits comparatively inferior localized injection ratio and hence meager locking efficiency, as displayed by their wider linewidths. In general, the spectral linewidths of each locked mode of Fig. 6(a), (b), and (c) multi-wavelength spectrums are found to be similar exhibiting mean values of ∼100, ∼130, and ∼170 pm, respectively, as shown in Fig. 7(c). This noticeable increase in mode linewidth with the number of locked modes appearing in the spectrum is possibly to compensate for the composite phase matching condition of each longitudinal modes simultaneously.

Another essential characteristic of a multi-wavelength laser is the requirement of a uniform free spectral range (FSR) or mode spacing across all the modes. This is also investigated in Fig. 7(c) by plotting the mode spacing variation across adjacent locked modes for all the wavelength spectrums of Fig. 6. Note that the mode spacing is measured as the difference between the central lasing wavelengths (calculated at the full-width-at-half-maximum) of the neighboring modes. A mode variation of ∼0.52±0.08 nm (583±70 GHz) is measured for the 4 comb lines source while the corresponding value for the 3 and 2 locked mode spectrums are ∼0.5±0.1 nm (551±92 GHz) and ∼0.6 nm (653 GHz), respectively, thus preserving the characteristics of multi-wavelength generation with appreciably small FSR variation. We strongly believe that proper optimization of the system, particularly via the deployment of piezo stages for external cavity tuning; an equidistant mode spacing with comparable mode linewidth multi-wavelength generation is feasible.

Next, we investigated the variation of SNR (ratio of the peak power of each mode to the ASE noise floor) and the peak power ratio across different multi-wavelength lasing emission of Fig. 6, and summarized the results in Fig. 7(d). The SNR is found to degrade as the number of modes in the multi-wavelength laser increases. For instance, the SNR for a single mode spectrum is measured to be ∼30 dB at 75 mA, attributed to the superior phase matching condition of the locked mode. This value subsequently decreased to ∼20 dB for the dual locked case and eventually to ∼13 dB for the 4 locked FP mode spectrum at 40 °C and 50 mA bias. This is ascribed, partly to a similar integrated power (∼10.3 mW) distribution among the four modes in the latter case compared to the former dual modes case, as displayed in Fig. 7(a), and to the phase matching condition,

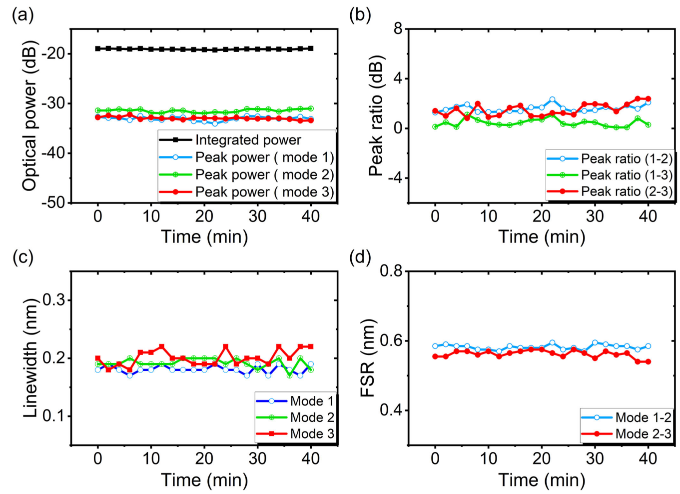

Fig. 8. Stability test of the multi-wavelength laser emission with 3 simultaneously locked modes, showing the time variation of (a) peak power of each mode and the total integrated power (arb. units), (b) peak power ratio across the modes, (c) linewidth of the modes, and (d) FSR across the modes.

which is quite rigorous in the latter case. On the other hand, peak power ratios are found to exhibit very close to 0 dB values in all the multi-wavelength spectrums suggesting almost equal peak powers across the modes of the spectrums. The minimum and maximum peak power ratios were found to be ∼0 and ∼0.6 dB, found between mode 2–3 and mode 1–3 in Fig. 6(d) and Fig. 6(c), respectively. This again affirms the quality of the generated multi-wavelength spectrums with flat-top and high SNR that is crucial in applications like WDM-VLC since any amplification would result in a consistent power levels across the modes thus negating incorporation of gain-flatting filters in the communication system.

C. Stability Analysis

Lastly, we analyzed the stability of the generated multiple wavelength FP modes to further support the potential deployment of the proposed self-injection locked based ECDL system in practical applications. Accordingly, we performed a short-term stability test on the 3 locked mode spectrum using the experimental setup shown in Fig. 1(a), where the optical powers, peak ratios, linewidths, and FSRs have been recorded at every 2 minutes time interval for over 40 minutes. The results are summarized in Fig. 8 with laser diode biased at 43 mA and operated at 20 °C. A variation of ±0.8 dB in the peak power of mode 1 is observed from Fig. 8(a) whereas the other modes were found to be very stable. Hence, the total integrated power of the system remained almost constant, which is vital in several applications. Fig. 8(b) and (c) shows minor fluctuations in the peak power ratio and mode linewidth across the three locked wavelength modes over time depicting a random trend, which suggests a slightly noisy system. Proper optimization of the system further (*i.e.,* external cavity length) should decrease these variations and hence the noise of the system considerably. Nevertheless, a variation of the peak power ratio across modes 1-2, 1-3, and 2-3 are ±0.5 dB, ±0.5 dB and ±0.7 dB, respectively, and the linewidth fluctuation of mode 1, 2, and 3 are measured to be ± 10 pm, ± 15 pm, and ± 20 pm. This suggests that modes 1 and 2 are more stable than mode 3 in general, which is further reflected in Fig. 8(d) that shows the variation in FSR across the three locked modes. While the variation of ± 10 pm is observed between modes 1-2, modes 2-3 exhibited a corresponding value of ± 20 pm. Nonetheless, overall, the system is found to be very stable, which indicates that the generated multi-wavelength emission qualifies as potential sub-carriers in WDM-VLC.

V. Conclusion

To summarize, a single and two stage self-injection locking ECDL arrangement with an InGaN/GaN green laser diode is developed to demonstrate a multi-wavelength and near single wavelength generation at $\sim$525 nm. Successful simultaneous locking of one to four FP modes with $\sim$0.5 nm FSR and up to $\sim$30 dB SNR is demonstrated. This first-of-its-kind visible multi-wavelength laser system exhibited mean $\sim$150 pm mode linewidth with similar peak and integrated power levels, and appreciably stable, particularly in terms of FP modes wavelength shift. Besides, an ultra-narrow near single wavelength linewidth of $\sim$34 pm is measured from two stage self-injection locked ECDL system with $\sim$20 dB SMSR. Our proposed schemes are compact, simple and cost-effective compared to other ECDL configurations, and in particular, power efficiency since a usable optical power as high as $\sim$65% of the diode laser power is achieved, thus addressing a plethora of multi-disciplinary field applications that require coherent single and multiple wavelength visible laser sources.

References

[1] R. Ana and M. Lopez-Amo, "Multi-wavelength fiber lasers," in *Current Developments in Optical Fiber Technology*, S. W. Harun, Ed. Rijeka, Croatia: InTech, 2013.

[2] T. J. Slight *et al.*, "Continuous-wave operation of (Al,In)GaN distributed-feedback laser diodes with high-order notched gratings," *Appl. Phys. Exp.*, vol. 11, no. 11, Nov. 2018, Art. no. 112701.

[3] Y. Chen, W. Lin, H. Chen, J. Shy, and H. Chui, "Single-frequency external cavity green diode laser," *IEEE Photon. J.*, vol. 9, no. 6, Dec. 2017, Art. no. 1507207.

[4] Y.-H. Chen, W.-C. Lin, J.-T. Shy, and H.-C. Chui, "Iodine-stabilized single-frequency green InGaN diode laser," *Opt. Lett.*, vol. 43, no. 1, pp. 126–129, Jan. 2018.

[5] M. Chi, O. B. Jensen, and P. M. Petersen, "Green high-power tunable external-cavity GaN diode laser at 515 nm," *Opt. Lett.*, vol. 41, no. 18, pp. 4154–4157, Sep. 2016.

[6] C. J. Hawthorn, K. P. Weber, and R. E. Scholten, "Littrow configuration tunable external cavity diode laser with fixed direction output beam," *Rev. Scientific Instrum.*, vol. 72, no. 12, pp. 4477–4479, Nov. 2001.

[7] A. Rolland, P. Li, M. Cassinerio, J. Jiang, and M. Fermann, "Precision visible comb from an Er fiber laser," presented at the Conf. Lasers and Electro-Optics, 2018, Paper JTh2A.185.

[8] Y. Yang *et al.*, "Four-wave mixing parametric oscillation and frequency comb generation at visible wavelengths in a silica microbubble resonator," *Opt. Lett.*, vol. 41, no. 22, pp. 5266–5269, Nov. 2016.

[9] C.-Y. Lin, Y.-C. Chi, C.-T. Tsai, H.-Y. Chen, and G.-R. Lin, "Two-color laser diode for 54-Gb/s fiber-wired and 16-Gb/s MMW wireless OFDM transmissions," *Photon. Res.*, vol. 5, no. 4, pp. 271–279, Aug. 2017.

[10] H.-Y. Wang, Y.-C. Chi, and G.-R. Lin, "Dual-mode laser diode carrier with orthogonal polarization and single-mode modulation for remote-node heterodyne MMW-RoF," *Opt. Lett.*, vol. 41, no. 20, pp. 4676–4679, Oct. 2016.

[11] G.-R. Lin *et al.*, "Long-cavity fabry–perot laser amplifier transmitter with enhanced injection-locking bandwidth for WDM-PON application," *J. Lightw. Technol.*, vol. 28, no. 20, pp. 2925–2932, Oct. 2010.

[12] G.-R. Lin *et al.*, "Comparison on injection-locked fabry–perot laser diode with front-facet reflectivity of 1% and 30% for optical data transmission in WDM-PON system," *J. Lightw. Technol.*, vol. 27, no. 14, pp. 2779–2785, Jul. 2009.

[13] L. Fan *et al.*, "High-purity 60 GHz band millimeter-wave generation based on optically injected semiconductor laser under subharmonic microwave modulation," *Opt. Express*, vol. 24, no. 16, pp. 18252–18265, Aug. 2016.

[14] M. Pochet, N. A. Naderi, Y. Li, V. Kovanis, and L. F. Lester, "Tunable photonic oscillators using optically injected quantum-dash diode lasers," *IEEE Photon. Technol. Lett.*, vol. 22, no. 11, pp. 763–765, Jun. 2010.

[15] M. A. Shemis *et al.*, "Broadly tunable self-injection locked InAs/InP quantum-dash laser based fiber/FSO/hybrid fiber-FSO communication at 1610 nm," *IEEE Photon. J.*, vol. 10, no. 2, Apr. 2018, Art. no. 7902210.

[16] M. A. Shemis *et al.*, "L-band quantum-dash self-injection locked multi-wavelength laser source for future WDM access networks," *IEEE Photon. J.*, vol. 9, no. 5, Oct. 2017, Art. no. 7905807.

[17] A. Hurtado, R. Raghunathan, I. D. Henning, M. J. Adams, and L. F. Lester, "Simultaneous microwave- and millimeter-wave signal generation with a 1310-nm quantum-dot-distributed feedback laser," *IEEE J. Sel. Topics Quantum Electron.*, vol. 21, no. 6, Nov. 2015, Art. no. 1801207.

[18] A. Hurtado *et al.*, "Tunable microwave signal generator with an optically-injected 1310 nm QD-DFB laser," *Opt. Express*, vol. 21, no. 9, pp. 10772–10778, May 2013.

[19] B. Janjua *et al.*, "Going beyond 4 Gbps data rate by employing RGB laser diodes for visible light communication," *Opt. Express*, vol. 23, no. 14, pp. 18746–18753, Jul. 2015.

[20] A. Sheetal and H. Singh, "5×10 Gbps WDM-CAP-PON based on frequency comb using OFDM with blue LD," *Opt. Quant. Electron.*, vol. 50, no. 12, Nov. 2018, Art. no. 446.

[21] S. H. Younus and J. M. H. Elmirghani, "WDM for high-speed indoor visible light communication system," in *Proc. 19th Int. Conf. Transparent Opt. Netw.*, 2017, pp. 1–6.

[22] M. Kong *et al.*, "10-m 9.51-Gb/s RGB laser diodes-based WDM underwater wireless optical communication," *Opt. Express*, vol. 25, no. 17, pp. 20829–20834, Aug. 2017.

[23] M. H. M. Shamim *et al.*, "Investigation of self-injection locked visible laser diodes for high bit-rate visible light communication," *IEEE Photon. J.*, vol. 10, no. 4, Aug. 2018, Art. no. 7905611.

[24] M. H. M. Shamim, T. K. Ng, B. S. Ooi, and M. Z. M. Khan, "Tunable self-injection locked green laser diode," *Opt. Lett.*, vol. 43, no. 20, pp. 4931–4934, Oct. 2018.

[25] C. M. Schultz, *Analysis and Mitigation of the Factors Limiting the Efficiency of High Power Distributed Feedback Diode Lasers*. Berlin, Germany: Technische Universität Berlin, 2013.

Md Hosne Mobarok Shamim received the B.Sc. degree in electrical and electronic engineering from the Islamic University of Technology, Dhaka, Bangladesh, in 2013, and the M.Sc. degree from the King Fahd University of Petroleum and Minerals, Dhahran, Saudi Arabia, in 2018. Currently, he is working toward the Ph.D. degree with McGill University, Montreal, QC, Canada. His research interest includes semiconductor lasers and supercontinuum sources. He is a recipient of McGill Engineering Doctoral Award.

Tien Khee Ng (SM'17) received the M.Eng. degree and the Ph.D. degree from Nanyang Technological University (NTU), Singapore, in 2001 and 2005, respectively. He was a Test Engineer with Hewlett-Packard Singapore (1997–1998), a Member of the Technical Staff with Tinggi Technologies (2004–2006), and a Research Fellow with NTU until 2009. He is a Senior Research Scientist with Ooi-Group, King Abdullah University of Science and Technology (KAUST), Thuwal, Saudi Arabia. As a Co-Principal Investigator responsible for innovation in MBE-grown nanostructures devices and in laser devices at the KACST Technology Innovation Center, KAUST, he realized wide-bandgap nitride quantum-confined and nanowires structures for light-emitters technology, optical wireless communications, and energy harvesting. He is a member of SPIE and a Senior Member of OSA.

Boon S. Ooi received the Ph.D. degree from the University of Glasgow, Glasgow, U.K., in 1994. He joined King Abdullah University of Science and Technology (KAUST), Thuwal, Saudi Arabia from Lehigh University, USA, in 2009. He is a Professor of electrical engineering with KAUST. His recent research is concerned with the study of III-Nitride based materials and devices, and lasers for applications, such as solid-state lighting, visible light, and underwater wireless optical communications, and energy harvesting devices. He has served on the technical program committee of CLEO, IPC, ISLC, and IEDM. He currently serves on the editorial board of *Optics Express* and IEEE PHOTONICS JOURNAL. He is a Fellow of OSA, SPIE, and IoP (U.K.).

Mohammed Zahed Mustafa Khan (SM'17) received the B.E. degree in electronics and communication from Osmania University, Hyderabad, India, in 2001, the M.S. degree in electrical engineering from the King Fahd University of Petroleum and Minerals (KFUPM), Dhahran, Saudi Arabia, in 2004, and the Ph.D. degree in electrical engineering from the King Abdullah University of Science and Technology (KAUST), Thuwal, Saudi Arabia, in 2013. Prior to joining KFUPM, he was a SABIC Postdoctoral Research Fellow with Photonics Laboratory, KAUST, from 2014–2015. His prior research involved developing numerical models for integrated optical device simulation. Currently, his research focus is on development of near infrared and visible semiconductor lasers and systems for applications in optical communications.